7-27-2015

Stratification of a population of intracranial aneurysms using blood flow metrics.

Rohini Retarekar
University of Iowa

Manasi Ramachandran
University of Iowa

Benjamin Berkowitz
University of Iowa

Robert E. Harbaugh
Penn State University

David Hasan
University of Iowa

See next page for additional authors

Authors
Rohini Retarekar, Manasi Ramachandran, Benjamin Berkowitz, Robert E. Harbaugh, David Hasan, Robert H. Rosenwasswer, Christopher S. Ogilvy, and Madhavan L. Raghavan

Published in final edited form as:
Comput Methods Biomech Biomed Engin. 2015 August ; 18(10): 1072–1082. doi: 10.1080/10255842.2013.869322

Stratification of a Population of Intracranial Aneurysms Using Blood Flow Metrics

Rohini Retarekar, Ph.D.[1], **Manasi Ramachandran, Ph.D.**[1], **Benjamin Berkowitz, B.S.E.**[1], **Robert E Harbaugh, M.D.**[2], **David Hasan, M.D.**[3], **Robert H Rosenwasser, M.D.**[4], **Christopher S Ogilvy, M.D.**[5], and **Madhavan L Raghavan, Ph.D.**[1]

[1]Department of Biomedical Engineering, University of Iowa, Iowa City, IA 52242

[2]Department of Neurosurgery, Penn State Milton S. Hershey Medical Center, Penn State University, Hershey, PA 17033

[3]Department of Neurosurgery, University of Iowa, Iowa City, IA 52242

[4]Department of Neurological Surgery, Jefferson University Hospital, Thomas Jefferson University, Philadelphia, PA 19107

[5]Department of Neurosurgery, Massachusetts General Hospital, Boston, MA 02114

Abstract

Indices of the intra-aneurysm hemodynamic environment have been proposed as potentially indicative of their longitudinal outcome. To be useful, the indices need to be used to stratify large study populations and tested against known outcomes. The first objective was to compile the diverse hemodynamic indices reported in the literature. Further, since morphology is often the only patient-specific information available in large population studies, the second objective was to assess how the ranking of aneurysms in a population is affected by the use of steady flow simulation as an approximation to pulsatile flow simulation even though the former is clearly non-physiological. Sixteen indices of aneurysmal hemodynamics reported in the literature were compiled and refined where needed. It was noted that in the literature, these global indices of flow were always time-averaged over the cardiac cycle. Steady and pulsatile flow simulations were performed on a population of 198 patient specific and 30 idealized aneurysm models. All proposed hemodynamic indices were estimated and compared between the 2 simulations. It was found that, steady and pulsatile flow simulations had a strong linear dependence ($r \geq 0.99$ for 14 indices; $r \geq 0.97$ for two others) and rank the aneurysms in an almost identical fashion ($\rho \geq 0.99$ for 14 indices; $\rho \geq 0.96$ for other two). When geometry is the only measured piece of information available, stratification of aneurysms based on hemodynamic indices reduces to being a physically grounded substitute for stratification of aneurysms based on morphology. Under such circumstances, steady flow simulations may just be as effective as pulsatile flow simulation for estimating most key indices currently reported in the literature.

Keywords

Computational Fluid Dynamics; Intracranial Aneurysms; Wall shear stress

Introduction

Simulations of blood flow in intracranial aneurysms (IA) have been reported for populations of human subjects [1-9]. It has been proposed that certain characteristics of blood flow in unruptured IAs may provide clues to their eventual outcome – whether they remain stable, grow and/or rupture. While visualizations of simulations may help us understand and gain insights into the nature of flow, to be of practical value (say, as a predictive factor of outcome), such simulations need to be quantified with scalar indices. These metrics may then be evaluated in adequately powered and appropriately chosen human subject populations. In the literature, blood flow simulations have been reported with varying degrees of assumptions. The results have been quantified with scalar indices that quantify diverse aspects of flow on a global basis. Such indices include those based on the distribution of wall shear stress[3-5], its spatial or temporal gradients[5], energy loss[7], pressure differentials[10], nature of inflow or outflow into aneurysm sac[1, 5, 6, 8] and prevalence of and nature of flow vortices[1, 5, 11]. We found about 20 such indices in the literature. The first objective of this study is to collect and summarize all reported indices of IA hemodynamics with improvements to their definitions where necessary.

Ultimately, the main use for such indices is for testing their prognostic value in human subject population. In the literature, most of these indices were computed based on pulsatile flow simulations in patient-specific aneurysms reconstructed from noninvasive volumetric imaging data. Although the simulations of transient blood flow seemingly provide in-depth information of intra-aneurysmal hemodynamics, the simulations are often computationally expensive and demand additional measurements such as the temporal variations in boundary conditions – an area where studies involving large populations inevitably make uniform population-wide assumptions. Moreover, in a large population study, the only patient specific information readily available is the morphology of aneurysm. Consequently, differences in hemodynamics indices within study populations have to merely be reflective of differences in morphological differences such as the angulation of the sac with respect to parent flow, the bottleneck effect at the neck of the sac, etc. Therefore, it is conceivable that if the primary objective is to stratify a population of aneurysms according to their hemodynamic behavior, a simpler and faster method of steady flow simulation can turn out to be as effective as transient flow simulation. Manageable computational cost will permit ever larger study populations to be accommodated into studies and consequently, greater statistical power in the testing of hypotheses. Of course, a steady flow simulation will not provide temporal information as pulsatile simulations and a comparison of the results will leave the former short. But do the loss of this additional information when employing steady flow simulation have any practical impact – say, in stratifying subjects any differently than that when pulsatile simulations are employed? This is the question motivating the second objective of this study. In this study, we compared the effectiveness of steady versus pulsatile flow simulations in stratifying aneurysms using two types of study populations: 1) a large population of patient-specific unruptured intracranial aneurysms with available sizes, shapes and locations; and 2) a population of idealized intracranial aneurysms spanning the common range of sizes, shapes and locations.

Methods

Hemodynamic Indices

A literature survey was performed to determine the indices that have been used to characterize cerebral aneurysm hemodynamics. Where necessary, we modified these existing indices and developed additional new ones. The indices were then organized within groups depending upon the nature of blood flow through the aneurysm they attempt to quantify:

A. Wall shear stress (WSS) based indices: WSS has long been proposed as a mechanobiological driver of wall remodeling [12]. To be effective as a prognostic indicator however, this spatially and temporally varying quantity should be reduced to an index. The following WSS related indices have been reported in the literature:

1. Temporally averaged, spatial mean WSS in the sac region[5], WSS_{ave}

2. Temporally averaged, spatial maximum WSS in the sac region[5], WSS_{max}

3. Temporally averaged, spatial 99th percentile WSS in the sac region, WSS_{99}. When large study populations are involved, this index may capture the essence of WSS_{max}, while avoiding the pitfalls of localized spikes due to model artifacts if any[13].

4. Low wall shear area, *LSA*: Under the premise that abnormally low WSS may promote aneurysmal growth [2] and therefore undesirable, the surface area covered by low WSS has been proposed as an index. However, what constitutes “abnormally low” is not consistent between investigators. Whereas Jou et al. and later Xiang et al. defined “abnormally low WSS” as less than 10% of mean parent vessel wall shear stress [3, 5], Cebral et al. defined “abnormally low WSS” as less than 1 standard deviation (SD) of the near vessel (vessels within 1 cm from the neck area) wall shear stress [6]. Of the two, the latter definition better accounts for the spread of WSS in the parent vessel while prescribing what is “abnormally low” (for e.g., for aneurysms at the siphon of the ICA, the parent vessel WSS likely spans a rather wide range such that even 10% of the mean may not be justifiably judged to be “abnormally low”). By employing parametric statistical estimates such as mean and standard deviation, both definitions make the presumption that WSS in the near vessel region is normally distributed (for e.g., the SD based definition may result in non-negative values for “abnormally low WSS” when the SD is higher than the mean, a not-so-uncommon occurrence in some parent vessels such as ICA with siphon in the computational domain). We submit that the best alternative is to use a non-parametric approach while accommodating the spread of WSS in the parent vessel. Hence, we define abnormally low WSS as less than the 15.87th percentile (the non-parametric equivalent of “mean-SD” in a normal distribution based on the “three sigma rule” or the “68-95-99.7 rule”) of WSS in the near vessel area. We submit that this improved definition will capture the abnormally low wall shear area efficiently in all

cases. Where the WSS distribution is indeed normally distributed, it will be the same as being lower than one SD from the mean. While we submit that this revised definition is conceptually sound, it would not be surprising if stratification of aneurysms based on it turns out to be no different than that by previous definitions for most cases.

5. Low shear concentration index (LSCI) is a new index we define here as the ratio of the average (temporal and spatial) shear stress in the low shear area (see definition for LSA above) over that in the entire aneurysm sac. This new definition is a modified version of low shear index defined by Cebral et al. [6]. LSI was defined as the "relative amount of the total shear force applied in regions of abnormally low WSS". The physical meaning of such an index and the mathematical definition proposed for it in their report are unclear to us and hence this modified definition.

6. High shear area (HSA): We propose a high shear area index as the area of aneurysm that is exposed to wall shear stress above 84.13^{th} percentile. Cebral et al.[6] had originally used a high shear area for calculating SCI (defined below), but defined it as the area of regions exposed to shear stress that is higher than mean+SD of WSS in the near vessel region. Our choice of 84.13^{th} percentile for delineating what is "high" is that it is the non-parametric equivalent of mean+SD in a normal distribution under the same rationale as that for defining "abnormally low" under LSA.

7. Shear concentration index (SCI): SCI, defined by Cebral et al. [6] is the ratio of the average (temporal and spatial) shear stress in the high shear area (see definition for HSA above) over that in the entire aneurysm sac. SCI is simply the high shear counterpart to LSCI.

8. Mean, Maximum and 99^{th} percentile WSS spatial gradient (WSSG): Xiang et al. [5], proposed mean WSSG to capture spatial non-uniformity in WSS. We include the maximum and 99^{th} percentile WSSG in the aneurysm sac under similar rationale as with its WSS counterpart. Respectively, these indices are $WSSG_{ave}$, $WSSG_{max}$ and $WSSG_{99}$.

9. Mean Oscillatory shear index (OSI_{ave}) proposed by Xiang et al.[5] captures the temporal directional change of WSS during the cardiac cycle reduced to a global index by spatial averaging. OSI_{ave} quantifies the temporal disturbance in flow in an aneurysm sac.

B. Energy based indices: As blood flows into the aneurysm, an energy loss occurs by virtue of its inertial and viscous effects and may be quantified by indices proposed by Cebral et al.[6]

1. Kinetic Energy Ratio (KER): This index quantifies the amount of kinetic energy in the aneurysm relative to the contiguous vasculature

2. Viscous Dissipation Ratio (VDR): Viscous dissipation is the rate at which the work done against viscous forces is irreversibly converted into internal

energy. This index measures the ratio of viscous dissipation in the aneurysm normalized by the viscous dissipation in the near vessel region.

C. Pressure differential based indices: Pressure in the wall regions is the loading on it that may drive its remodeling and/or rupture. We define in this context, the temporally averaged spatial mean (DP_{ave}) and spatial maximum (DP_{max}) difference in pressure between the aneurysm and near vessel. While physically intuitive, caution is warranted with use of these indices because pressure computations in CFD analyses, especially with the use of constant pressure outlet conditions, are not necessarily reliable[14, 15].

D. Intra-sac flow based indices: The nature of blood flow inside the aneurysm sac is determined by the sac morphology and how it relates to its contiguous vasculature. The following indices quantify key aspects of such flow:

1. Inflow concentration index (ICI): Defined by Cebral et al., [6] this quantifies the degree of concentration of inflow jet entering the sac relative to the parent vessel.

2. Residence time (RT): We define here, RT as the average of the time spent by all particles entering the aneurysm. To calculate this index, time-averaged streamtraces may be plotted in the aneurysm sac. Using the velocity and distance information from the streamtraces, the time spent by an average particle may be calculated.

3. Vortex length (VL): As blood flows into the aneurysm, it undergoes recirculation, swirling and exhibits 3-D vortices. Traditionally, vorticity information is obtained from a representative cross sectional plane. However, this method is subjective and might prove erroneous if the vortices inside the aneurysm are out of plane. We propose VL as a new index to quantify the spread of the recirculation region. Vortex length tracks the centerline of spiraling flow using the critical point theory. Critical points were defined by Chong et al. [16] as “points where the streamline slope is zero and the velocity is zero relative to an appropriate observer”. According to the critical point theory, the Eigen values and Eigen vectors of the rate of deformation tensor evaluated at a critical point define the flow pattern about that point. For one real and a pair of complex conjugate Eigen values, the flow forms a spiral-saddle pattern [17]. VL is the length of the vortex centerline and quantifies the extent of recirculation in the aneurysm. Incidentally, Raschi et al. [18] recently reported the use of vortex coreline for cerebral aneurysms whose length is what we propose here as a quantitative metric.

While we have included almost all indices proposed in the literature, some exceptions are worth noting.

- Normalizations of WSS and WSSG based indices with respect to their near vessel averages have been proposed by Xiang et al. [5]. We did not propose normalization with parent vessels for these indices because the depth of existing literature on

WSS-related vessel wall pathology may permit their direct interpretation. But we concede it may be a prudent alternative considering that most other indices proposed above are indeed normalized with respect to the near vessel region.

- Qian et al.[7] proposed energy loss as an index. They calculated it as the difference in energy loss between inlet and outlet points in the near vessel region with and without the aneurysm. That quantity is not included here, as KER likely already quantifies the predominant kinetic energy portion of energy loss.
- Baharoglu et al.[8] proposed shear jet zone size and velocity jet distance to tip as indices of aneurysm in-flow jet characteristics. They are indices of the location (distance from neck or dome) of the median value for WSS and for inflow velocity respectively. However, since the neck point and dome point for an arbitrarily-shaped aneurysm is difficult to define; we did not propose them here. As our ability to characterize sac morphology improves (recent advances do point the way [19]), these indices may yet become objectively calculable.
- And finally, while pulsatile flow simulations result in temporally varying quantities, in the literature, the above indices are calculated after temporal averaging. However, some exceptions exist. Shojima et al.[4] and Jou et al.[3] used peak systolic and end-diastolic instances for calculating indices.

Study population

Two independent populations of brain aneurysm models were used in this study to evaluate the indices and compare the practical effectiveness of steady versus pulsatile simulations: 1) Image-based models from human subjects and 2) idealized models from a population-average brain arterial network model. The human subjects study population provide realism to the comparisons while, the idealized model population provide additional insights without any inherent study sample biases in locations, sizes and shapes.

Human subjects—Scan data for 198 unruptured aneurysms that were diagnosed at 4 different clinical centers (The Penn State Hershey Medical Center, Thomas Jefferson University Hospital, Harvard University-Massachusetts General Hospital and The University of Iowa Hospitals and Clinics) were obtained. Three-dimensional models of aneurysms and their contiguous vasculature were reconstructed using the level set segmentation techniques implemented in the open-source software "*Vascular Modeling toolkit*"(VMTK) [20] (Figure 1). The non-shrinking filters by Taubin implemented in VMTK were used to smooth the segmented model. Table 1 provides the distribution of these aneurysms according to their location in the cerebral vasculature.

Idealized models—30 idealized models of cerebral aneurysms and their contiguous vasculature were created in Rhinoceros 3D. Use of additional idealistic models in the study provided a control on the morphological aspect of comparison. The idealized models were created by placing aneurysm sacs in a head and neck arterial network model developed in-house with population averaged dimensions [21] (Figure 2) and truncating it to the flow-relevant domains. Specifically, the 30 sacs were a result of perturbing the following aspects of morphology:

- Location: Internal Carotid Artery, Basilar Tip and Anterior Communicating Artery
- Size Ratio (Height of aneurysm/ Diameter of parent vessel)[22]: 1, 2 and 3
- Shape: Spherical, prolate ellipsoid and oblate ellipsoid
- Daughter Sac Models: For spherical ICA aneurysm of size ratio 2, three additional models of daughter sac bearing aneurysms were created. Size of the daughter sac was chosen to be 40%, 50% and 60% of the aneurysm diameter in the three models.

Choice of these locations was made to include both anterior and posterior circulation in the flow analysis. Precise location for attachment of daughter sac was determined after consultation with a physician to ensure representativeness of the general population.

CFD analysis

Meshing of the image based models was performed using VMTK and *Gambit* (Ansys Inc., Lebanon, NH). Gambit's curvature size function was used to obtain a finer mesh in regions of larger curvature such as the aneurysm. In order to capture the boundary layer with better accuracy, prism elements were used to mesh the near wall region. The mesh densities varied from 0.5 to 8 million tetrahedral elements. Flow waveform by Ford et al.[23] was used to specify the inlet velocity for pulsatile flow analysis. The time-averaged flow value was used to specify inlet velocity in steady flow analysis. Constant pressure boundary condition was specified at the outlets. In the pulsatile flow analysis, 2 cardiac cycles were run for each case with a time step size of 0.001s (300 iterations/time-step) and a time period of 0.9 seconds. Solution from the second cardiac cycle was used for calculation of indices. Meshing of the 30 idealized models (27 models with all combinations of location, size ratio and shape with the 3 models with daughter sacs) was performed in Gambit with additional refinement of the aneurysm region. Mesh density for these models varied from 0.95 to 1.45 million tetrahedral elements. In order to specify velocity waveforms at the inlets, descriptive statistics of the internal carotid waveform presented by Ford et al. [23] were fitted to Fourier series using a Matlab program. For aneurysms positioned at locations other than ICA, the waveform was scaled such that the temporally averaged flow matches the population averaged value reported in literature. The time-averaged flow value was used to specify inlet velocity in steady flow analysis. Since, in the idealized models, the number of vessels remained constant across a given perturbation of aneurysm morphology, outflow boundary condition was specified by using flow rate values published in literature [24-31]. The inlet and outlet boundary conditions were adjusted down to account for the small amounts of flow through any small vessels which are not included in the models [32]. In the pulsatile flow analysis, 3 cardiac cycles were run for each case with a time step size of 0.001s (200 iterations/time-step) and solution from the third cardiac cycle was used. For the models in both study populations, the inlet was extended by adding a straight cylindrical tube so as to recreate the fully developed flow condition. Flow simulations were performed using the commercial software *Fluent* (Ansys Inc., Lebanon, NH). Blood was assumed to be a Newtonian, incompressible fluid. No-slip boundary condition was used. The "Semi-implicit method for pressure linked equations" scheme was used for pressure velocity coupling. Standard pressure discretization and first order momentum discretization was performed. All simulations used a convergence criterion of $1*10^{-6}$.

Statistical Analysis

Hemodynamic indices computed from steady flow simulations were compared to their time-averaged counterparts from pulsatile flow analysis using three statistical metrics. The Pearson product-moment correlation coefficient ($-1 \le r \le 1$) was used as a measure of the strength of linear dependence between the two approaches based on each index. When r=1, one method consistently scales up or scales down the indices within a study population compared to the other method (that is, the results from one method may be obtained from the other with a constant scale factor). The Spearman's rank correlation coefficient ($-1 \le \rho \le 1$) was used as a metric of the similarity in rank between two analysis – i.e., how they rank (and hence stratify) the aneurysms in the study population based on a given index. If the two analyses render an identical ranking order for the aneurysm population, then $\rho = 1$. Slope of the best-fit linear regression (with intercept =0) was used as the third comparison metric in this study ($-\infty \le k \le \infty$). If the value of an index calculated from pulsatile flow analysis is identical to its steady counterpart, then k =1. The Pearson's correlation assesses the level of numerical redundancy between estimates from two analyses. The Spearman's correlation assesses the impact any existing redundancies will have in clinical trial-type studies where hypotheses on rupture risk induced by abnormal hemodynamics are tested. ρ therefore is the metric directly relevant to our goal, but *r* and to an extent k, provide additional insight. As a subjective comparison, the spatial distribution of WSS from steady simulation was visually compared with time-averaged WSS from pulsatile simulation.

Results

Flow simulations converged for all but 5 cases. Models that did not meet the convergence criterion were excluded from the statistical comparison. All hemodynamic indices proposed above were computed for patient-specific models under steady and pulsatile conditions. WSS distributions and streamlines were found to be near identical between steady flow simulations versus time-averaged pulsatile flow simulations (see Figure 3 for representative illustrations). All indices showed a linear relationship between steady flow-based and pulsatile flow-based estimations (see Figure 4) with a very strong correlation and near-identical ranking (Table 2).

Discussion

There is increasing interest in assessing what role, if any, that hemodynamics in aneurysm may play in their natural history. So it is important to collect and compile the various global quantitative indices that capture the spatially and temporally variant flow characteristics. We believe we have done that in this study. The second aim of this study was to assess if it is possible to get the same ranking of a population of patient-specific aneurysms based on the aneurysmal hemodynamic environment using steady flow simulation as would be obtained from pulsatile flow simulation when population-wide assumptions are inevitably made about inlet and outlet flow conditions and material properties. At the outset, steady flow simulation may seem to be a dubious substitute for pulsatile flow simulation since we know the flow is indeed pulsatile and temporal variations do exist within a cardiac cycle. Indeed, if we are trying to understand aneurysmal flow phenomenon, pulsatile flow is indispensable. But, if

we are trying to distinguish, stratify or rank patient-specific aneurysms based on their flow characteristics – and this is often the case in many reported studies [1-3, 5, 6, 8, 10] – let us be careful not to confuse what we know happens inside the body with what we can reliably learn from modeling it with limited patient-specific information. Two key issues need to be considered in that context. One, we often tend to know little to nothing about the boundary conditions (inlet velocity profiles, outlet impedances) on a patient-specific basis. This forces us to make population-wide assumptions on such conditions (e.g., on temporal variation of inlet velocity and outlet impedance) making pulsatile flow modeling more of an unknown devil than steady flow modeling. And two, what we seek from these studies is not the actual results (such as value of WSS_{ave}), but rather how they differ among patients being evaluated. If the only measured difference between these patient-specific simulations is in the geometry and not in other aspects of the simulation, then the differences among patients in indices attained from pulsatile flow simulations may not (perhaps even should not) be different whether it is based on steady or pulsatile flow conditions. Some reported findings are indeed consistent with this assertion. Mantha et al.[33] identified common features of large scale flow patterns in 6 cerebral aneurysms using both steady and pulsatile flow simulations. Their results indicated that the basic flow pattern remains unchanged under steady state and pulsatile flow conditions. Geers et al.[34] compared steady-state to transient simulations of two patient specific intracranial aneurysms by conducting experiments examining the effect of flow rate waveform. Their study reported that the hemodynamic environment obtained from steady state simulation was similar to that obtained from a transient simulation. Cebral et al. [6] in their study with 210 patient specific cerebral aneurysms found that indices based on steady flow simulations distinguished ruptured from unruptured groups as effectively as pulsatile flow simulations.

The results reported here are consistent with the above mentioned studies. Since the key goal is the ranking of aneurysms within a population, the Spearman coefficient (ρ) is the most appropriate metric. Clearly, in all indices compared, ρ was almost 1, suggesting that in this large population, a steady flow simulation is as effective as a pulsatile flow simulation in stratifying aneurysms based on the indices reported. But the agreement goes deeper than that. That the Pearson coefficient (r) was also close to 1 suggests that steady flow based estimates consistently scales up or down those from pulsatile flow. Taken together, the results suggest that steady flow is about as effective for stratifying aneurysms based on the indices we have assessed when vessel and sac morphology is the only patient-specific information available within a population being studied. This is also conformed in the idealized study population. On occasion, some outliers may be noted such as some data points for VL and LSA. Although the correlation coefficients are slightly lower for VL and RT as compared to the other indices, the values for r and ρ are above 0.95. Since they are new indices, their robustness has not been established yet. It is speculated that it may be the reason for the slightly lower values. But for these few cases, there is little deviation from the overall finding. In the idealized models, some ACOM models did show apparent differences (see Fig.3 (f)), but these did not manifest in any significant manner on the stratification itself (ρ =0.99 for WSS_{ave}).

One could wonder if these findings are simply a result of using time-averaged estimates for the pulsatile simulations and whether differences may start to appear when indices are defined at the peak-systolic or end-diastolic time points. We concede that this study does not offer sufficient insights on that question. But as we note earlier, the fact remains that indices proposed in the mainstream literature are predominantly those that are time-averaged over the cardiac cycle. This is grounded in the notion that long-term changes to the aneurysm wall tissue pathology from blood flow characteristics are likely the result of “chronic”, not “acute” events. That is, flow characteristics that are spread out over a time period may matter more than characteristics that occur in short bursts – the use of time averaged indices (as opposed to peak-systolic ones) are consistent with this. Nevertheless, we concede that if future studies were to find that, metrics based on instantaneous flow characteristics such as peak-systolic WSS are important, steady flow simulation may not be necessarily sufficient. In such a case however, issues we have not satisfactorily addressed in this study may take forefront such as, mesh refinement. As is well known, an endlessly increasing mesh refinement is likely to result in an ever-increasing set of new insights into the flow characteristics. How dense should the refinement be before other assumptions such as ignoring the formed elements in blood and the associated non-Newtonian characteristics start to affect the simulations remains unclear. Therefore, the findings in this study that steady flow simulation may be sufficient for stratification of aneurysm in a population should be confined to time-averaged indices. Another limitation of the current study is that not all indices could be compared between steady and pulsatile flow simulations. OSI is one such pulsatile index with no direct steady-flow counterpart because temporal variation is in its very definition. However, the temporal gradients in flow characteristics that OSI quantifies are mainly determined by the temporal variations in the inlet velocity waveform – a presumed quantity that is uniformly applied within a study population. So this limitation does not overwhelm the validity of our case regarding the utility of steady flow simulation. On the other hand, in a large population study with morphology being the only measured differentiator among study subjects, Xiang et al. [5] found OSI was an independent discriminant of rupture status. This suggests that OSI may be affected by morphology in ways that aren’t captured by any of the steady flow indices. Clearly the effect of morphological characteristics on OSI independent of presumed temporal variations in the inlet waveform needs further study. Other assumptions such as use of rigid wall, Newtonian and incompressible fluid assumptions are common in the literature. The mesh resolution used in this study (about 0.15 mm element size and 1.5 million elements on average) are consistent with the literature [5, 6, 14] and consistent with the resolution of image data available to us for patient-specific geometric reconstruction. Still the optimal mesh resolution for assessing aneurysmal hemodynamics remains unknown and a matter of debate. And finally, we fail here to accommodate unsteady flow aspects that may occur under steady flow inlet and outlet boundary conditions, again an area of study as yet poorly understood.

In conclusion, we have reported here a broad collection of indices of blood flow in intracranial aneurysms with refinements where necessary. And we have shown that, to the extent we focus on time-averaged indices, and to the extent that we make consistent assumptions on inlet and outlet flow conditions for aneurysms (as has been done by

previously reported relevant studies), the ranking of aneurysms in a population will likely be no different whether we employ steady or pulsatile flow simulations. This is consistent with the fact that hemodynamics based stratification is but a physically grounded proxy for distinguishing aneurysms based on morphology – which is really the only measured piece of information that is known to be different between the aneurysms in this and in many patient population studies. We caution however that our claim here should not be misinterpreted as a broad claim about steady flow simulations being an effective substitute for pulsatile flow simulations under any given study goal or boundary conditions. Certainly, if the goal is to gain insights about the nature of flow in an aneurysm, to understand how it affects pathology, or to evaluate how it is affected by intervention and placement of an implant, then pulsatile flow simulations may well be indispensable.

Acknowledgements

This work was supported by the National Institute of Health (#R01 HL083475). It was also supported in part by the National Science Foundation through Teragrid resources provided by NCSA under (#TG-CTS100061). The authors would like to thank Anna Hoppe (University of Iowa) for her support in this work.

References

1. Cebral JR, Castro MA, Burgess JE, Pergolizzi RS, Sheridan MJ, Putman CM. Characterization of cerebral aneurysms for assessing risk of rupture by using patient-specific computational hemodynamics models. American Journal of Neuroradiology. 2005; 26(10):2550–2559. [PubMed: 16286400]
2. Boussel L, Rayz V, McCulloch C, Martin A, Acevedo-Bolton G, Lawton M, Higashida R, Smith WS, Young WL, Saloner D. Aneurysm growth occurs at region of low wall shear stress: patient-specific correlation of hemodynamics and growth in a longitudinal study. Stroke. 2008; 39(11): 2997–3002. [PubMed: 18688012]
3. Jou LD, Lee DH, Morsi H, Mawad ME. Wall shear stress on ruptured and unruptured intracranial aneurysms at the internal carotid artery. AJNR Am J Neuroradiol. 2008; 29(9):1761–7. [PubMed: 18599576]
4. Shojima M, Oshima M, Takagi K, Torii R, Hayakawa M, Katada K, Morita A, Kirino T. Magnitude and role of wall shear stress on cerebral aneurysm: computational fluid dynamic study of 20 middle cerebral artery aneurysms. Stroke. 2004; 35(11):2500–5. [PubMed: 15514200]
5. Xiang J, Natarajan SK, Tremmel M, Ma D, Mocco J, Hopkins LN, Siddiqui AH, Levy EI, Meng H. Hemodynamic-morphologic discriminants for intracranial aneurysm rupture. Stroke. 2011; 42(1): 144–52. [PubMed: 21106956]
6. Cebral JR, Mut F, Weir J, Putman C. Quantitative characterization of the hemodynamic environment in ruptured and unruptured brain aneurysms. AJNR Am J Neuroradiol. 2011; 32(1): 145–51. [PubMed: 21127144]
7. Qian Y, Takao H, Umezu M, Murayama Y. Risk Analysis of Unruptured Aneurysms Using Computational Fluid Dynamics Technology: Preliminary Results. American Journal of Neuroradiology. 2011; 32(10):1948–1955. [PubMed: 21903914]
8. Baharoglu MI, Schirmer CM, Hoit DA, Gao BL, Malek AM. Aneurysm inflow-angle as a discriminant for rupture in sidewall cerebral aneurysms: morphometric and computational fluid dynamic analysis. Stroke. 2010; 41(7):1423–30. [PubMed: 20508183]
9. Valencia, A.; Munizaga, J.; Rivera, R.; Bravo, E. Numerical investigation of the hemodynamics in anatomically realistic lateral cerebral aneurysms. IEEE; 2010.
10. Ma, B. Biomedical Engineering. University of Iowa; Iowa City: 2004. Modeling the geometry, hemodynamics and tissue mechanics of cerebral aneurysms.

11. Mulder G, Bogaerds ACB, Rongen P, van de Vosse FN. On automated analysis of flow patterns in cerebral aneurysms based on vortex identification. Journal of Engineering Mathematics. 2009; 64(4):391–401.
12. Malek AM, Alper SL, Izumo S. Hemodynamic shear stress and its role in atherosclerosis. JAMA: the journal of the American Medical Association. 1999; 282(21):2035–2042.
13. Speelman L, Bosboom E, Schurink G, Hellenthal F, Buth J, Breeuwer M, Jacobs M, van de Vosse F. Patient-specific AAA wall stress analysis: 99-percentile versus peak stress. European Journal of Vascular and Endovascular Surgery. 2008; 36(6):668–676. [PubMed: 18851924]
14. Cebral J, Mut F, Raschi M, Scrivano E, Ceratto R, Lylyk P, Putman C. Aneurysm rupture following treatment with flow-diverting stents: computational hemodynamics analysis of treatment. American Journal of Neuroradiology. 2011; 32(1):27–33. [PubMed: 21071533]
15. Fiorella D, Sadasivan C, Woo H, Lieber B. Regarding “Aneurysm Rupture Following Treatment with Flow-Diverting Stents: Computational Hemodynamics Analysis of Treatment”. American Journal of Neuroradiology. 2011; 32(5):E95–E97. [PubMed: 21511857]
16. Chong M, Perry A, Cantwell B. A general classification of three-dimensional flow fields. Physics of Fluids. 1990; 2:408–420.
17. Sujudi, D.; Haimes, R. Identification of swirling flow in 3D vector fields. Citeseer; 1995.
18. Raschi M, Mut F, Byrne G, Putman CM, Tateshima S, Viñuela F, Tanoue T, Tanishita K, Cebral JR. CFD and PIV analysis of hemodynamics in a growing intracranial aneurysm. International Journal for Numerical Methods in Biomedical Engineering. 2012
19. Piccinelli M, Steinman DA, Hoi Y, Tong F, Veneziani A, Antiga L. Automatic neck plane detection and 3D geometric characterization of aneurysmal sacs. Ann Biomed Eng. 2012; 40(10): 2188–211. [PubMed: 22532324]
20. Antiga, L.; Steinman, D. The vascular modeling toolkit. 2008.
21. Raghavan, ML. Interactive computer model of cerebral vasculature; Annual Meeting, Biomedical Engineering Society; Pittsburgh, PA. 2009;
22. Dhar S, Tremmel M, Mocco J, Kim M, Yamamoto J, Siddiqui AH, Hopkins LN, Meng H. Morphology parameters for intracranial aneurysm rupture risk assessment. Neurosurgery. 2008; 63(2):185. [PubMed: 18797347]
23. Ford MD, Alperin N, Lee SH, Holdsworth DW, Steinman DA. Characterization of volumetric flow rate waveforms in the normal internal carotid and vertebral arteries. Physiol Meas. 2005; 26(4): 477–88. [PubMed: 15886442]
24. Martin PJ, Evans DH, Naylor AR. Measurement of blood flow velocity in the basal cerebral circulation: advantages of transcranial color-coded sonography over conventional transcranial Doppler. J Clin Ultrasound. 1995; 23(1):21–6. [PubMed: 7699089]
25. Schoning M, Walter J, Scheel P. Estimation of cerebral blood flow through color duplex sonography of the carotid and vertebral arteries in healthy adults. Stroke. 1994; 25(1):17–22. [PubMed: 8266366]
26. Enzmann DR, Ross MR, Marks MP, Pelc NJ. Blood flow in major cerebral arteries measured by phase-contrast cine MR. AJNR Am J Neuroradiol. 1994; 15(1):123–9. [PubMed: 8141043]
27. Marks MP, Pelc NJ, Ross MR, Enzmann DR. Determination of cerebral blood flow with a phase-contrast cine MR imaging technique: evaluation of normal subjects and patients with arteriovenous malformations. Radiology. 1992; 182(2):467–76. [PubMed: 1732966]
28. Obata T, Shishido F, Koga M, Ikehira H, Kimura F, Yoshida K. Three-vessel study of cerebral blood flow using phase-contrast magnetic resonance imaging: effect of physical characteristics. Magn Reson Imaging. 1996; 14(10):1143–8. [PubMed: 9065904]
29. Bogren HG, Buonocore MH, Gu WZ. Carotid and vertebral artery blood flow in left- and right-handed healthy subjects measured with MR velocity mapping. J Magn Reson Imaging. 1994; 4(1): 37–42. [PubMed: 8148554]
30. Kashimada A, Machida K, Honda N, Mamiya T, Takahashi T, Kamano T, Osada H. Measurement of cerebral blood flow with two-dimensional cine phase-contrast mR imaging: evaluation of normal subjects and patients with vertigo. Radiat Med. 1995; 13(2):95–102. [PubMed: 7667516]
31. Valdueza JM, Balzer JO, Villringer A, Vogl TJ, Kutter R, Einhaupl KM. Changes in blood flow velocity and diameter of the middle cerebral artery during hyperventilation: assessment with MR

and transcranial Doppler sonography. AJNR Am J Neuroradiol. 1997; 18(10):1929–34. [PubMed: 9403456]

32. Fahrig R, Nikolov H, Fox AJ, Holdsworth DW. A three-dimensional cerebrovascular flow phantom. Med Phys. 1999; 26(8):1589–99. [PubMed: 10501059]
33. Mantha AR, Benndorf G, Hernandez A, Metcalfe RW. Stability of pulsatile blood flow at the ostium of cerebral aneurysms. Journal of biomechanics. 2009; 42(8):1081–1087. [PubMed: 19394943]
34. Geers AJ, Larrabide I, Morales HG, Frangi AF. Comparison of steady-state and transient blood flow simulations of intracranial aneurysms. Conf Proc IEEE Eng Med Biol Soc. 2010; 2010:2622–5. [PubMed: 21096183]

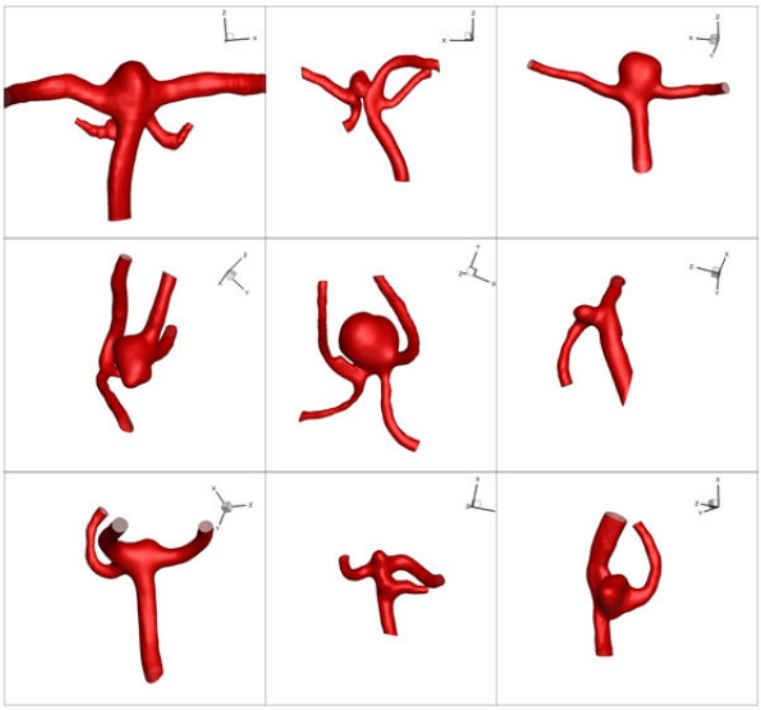

Figure 1.
Three dimensional models for 9 representative cases in the human subject population.

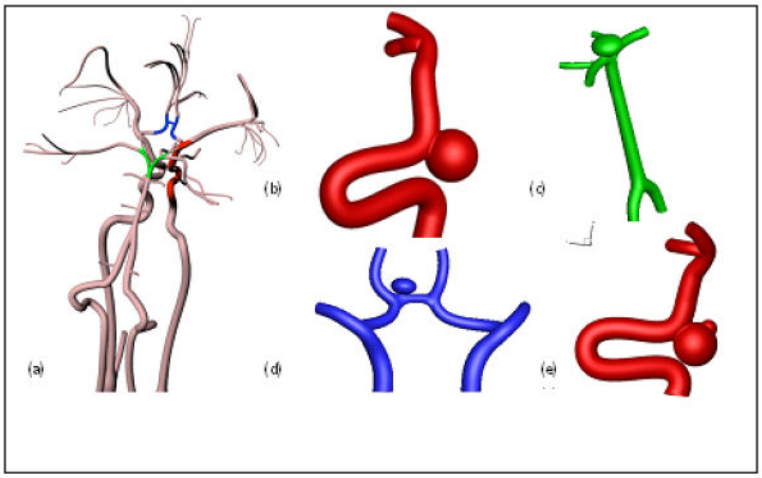

Figure 2.
(a) Complete circle of Willis model. Representative truncated model used for CFD simulations: (b) ICA aneurysm (c) Basilar aneurysm (d) ACOM aneurysm and (e) Daughter sac bearing ICA aneurysm

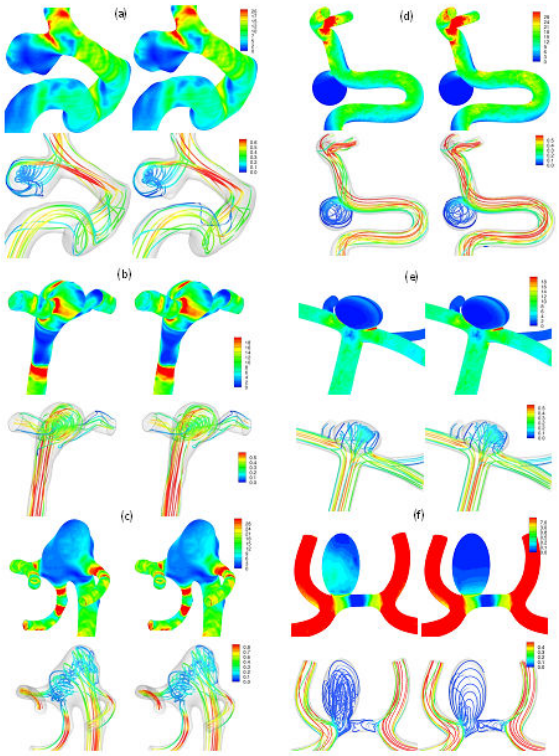

Figure 3.
WSS distribution and streamlines from steady and pulsatile flow simulations for 3 patient specific aneurysm models (a, b and c) and 3 idealized aneurysm models (d, e and f)

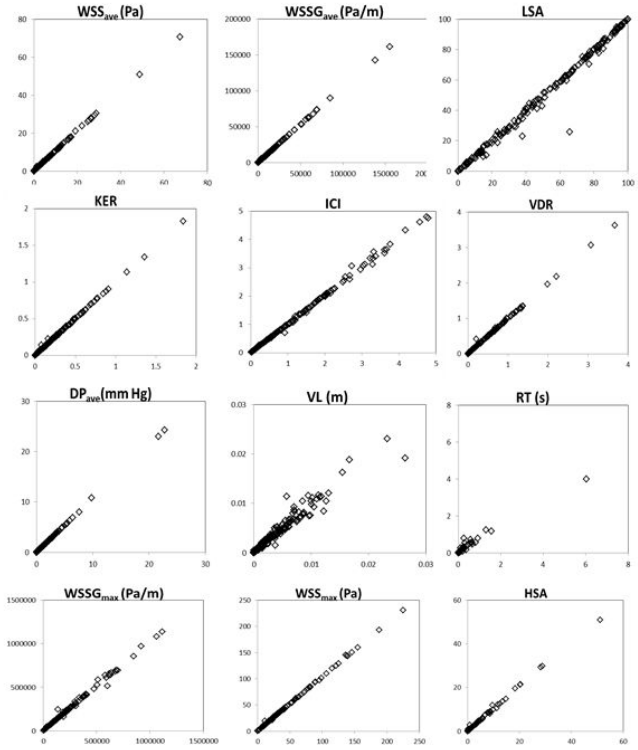

Figure 4.

Correlation between steady (x-axis) and pulsatile (y-axis) flow analysis of 193 patient specific aneurysms

Table 1

Distribution of aneurysms according to location

Location	Number of Aneurysms
Internal Carotid Artery (ICA)	67
Middle Cerebral Artery (MCA)	57
Anterior Communicating Artery (Acomm)	24
Basilar	10
Anterior Cerebral Artery (ACA)	15
Ophthalmic Artery (Ophth)	8
Posterior Cerebral Artery (PCA)	3
Posterior Communicating Artery (Pcomm)	6
Vertebral	2
Superior Cerebellar Artery (SCA)	3
Periophthalmic Artery (Periophth)	1
Posterior Inferior Cerebellar Artery (PICA)	2

Table 2
Statistical metrics for all hemodynamic indices

Index	Pearson Correlation (r)	Spearman Correlation (ρ)	Slope (k)
WSS_{ave}	0.9998	0.9992	1.0505
WSS_{max}	0.9997	0.9983	1.0320
WSS_{99}	0.9998	0.9994	1.0395
LSA	0.9948	0.9954	0.9990
HSA	0.9987	0.9908	1.0208
LSCI	0.9931	*0.9917	0.9857
SCI	0.9943	*0.9931	0.9139
$WSSG_{ave}$	0.9998	0.9991	1.0471
$WSSG_{max}$	0.9975	0.9981	1.0236
$WSSG_{99}$	0.9997	0.9991	1.0362
KER	0.9994	0.9983	0.9923
VDR	0.9993	0.9988	0.9874
DP_{ave}	0.9999	0.9995	1.0676
DP_{max}	0.9997	0.9987	1.0690
ICI	0.9991	0.9994	1.0110
VL	0.9713	0.9841	0.9292
RT	0.9752	0.9644	0.6777

* indicates that for some subjects the value of these indices were indeterminate and therefore they were not included in the Spearman Correlation calculation